IOPscience iopscience.iop.org

Home Search Collections Journals About Contact us My IOPscience

Electrical transport properties and magnetoresistance of $LaMn_{1-x}M_xO_{3+\delta}$ substituted with diamagnetic ions (M = Li, Mg, Ti)

This article has been downloaded from IOPscience. Please scroll down to see the full text article.

2000 J. Phys.: Condens. Matter 12 7747

(http://iopscience.iop.org/0953-8984/12/35/310)

View the table of contents for this issue, or go to the journal homepage for more

Download details:
IP Address: 171.66.16.221
The article was downloaded on 16/05/2010 at 06:44

Please note that terms and conditions apply.

J. Phys.: Condens. Matter **12** (2000) 7747–7758. Printed in the UK PII: S0953-8984(00)13066-8

Electrical transport properties and magnetoresistance of $LaMn_{1-x}M_xO_{3+\delta}$ substituted with diamagnetic ions (M = Li, Mg, Ti)

T R N Kutty and John Philip
Materials Research Centre, Indian Institute of Science, Bangalore 560 012, India

Received 5 April 2000, in final form 14 June 2000

Abstract. Substitution of aliovalent diamagnetic ions with fixed valence states (Li^+, Mg^{2+} and Ti^{4+}) at the Mn site in $LaMnO_3$ ($LaMn_{1-x}M_xO_{3+\delta}$) drastically decreases the room temperature resistivity (from ∼368 to ∼10 Ω cm). The concentration of Mn^{4+} ions increases with increase in diamagnetic addition. The presence of diamagnetic ions in $LaMnO_3$ samples shows low values of δ (0–0.045) in comparison to $LaMnO_{3+\delta}$ ($\delta = 0$–0.26). Therefore, the cation vacancies (La, Mn) in the La and Mn sublattices will be much lower than that of $LaMnO_{3+\delta}$; consequently the scattering of holes at the vacancies will be reduced, resulting in lower resistivity. There is no transition to metallic state at low temperatures even for samples with large hole concentration as in the case of $LaMn_{0.8}Mg_{0.2}O_{3+\delta}$. However, there is a transition from the para- to ferromagnetic state. In resistivity characteristics, the high temperature region satisfies the small polaron model and the activation energy calculated is less than 0.3 eV. Thermopower measurements exhibit a change in behaviour at low temperatures, which is not observed in resistivity curves. Magnesium added samples ($LaMn_{0.8}Mg_{0.2}O_{3+\delta}$) show a large negative magnetoresistance (MR) coefficient (0.8) at low magnetic fields ($H = 1$ T) and the MR increases with Mg concentration ($x = 0.05$–0.2). Samples treated at low partial pressures of oxygen at 1050–1300 K display large variation in resistivity and MR due to the reduction in holes.

1. Introduction

Stoichiometric $LaMnO_3$ is a well known antiferromagnetic insulator. The magnetic moments at the Mn sites are ferromagnetically coupled in planes that alternate spin orientation and this is known as A-phase antiferromagnetism [1]. In this structure, $Mn^{3+}(3d^4)$ is a Jahn–Teller ion surrounded by six oxygen atoms and the Jahn–Teller distortion reduces the electronic energy by splitting the localized three t_{2g} levels and two e_g levels. However, oxygen excess $LaMnO_{3+\delta}$ is reported to exhibit ferromagnetism at low temperature. $LaMnO_{3+\delta}$ is ferromagnetic (FM) when δ is greater than 0.1 [2–4]. The excess oxygen cannot be accommodated interstitially in the lattice; thus it is postulated that there exist equal amounts of La and Mn vacancies [5]. The aim of the present work is to study the modification in electrical conductivity and magnetoresistance (MR) effect of $LaMnO_{3+\delta}$, after reducing the δ value by adding diamagnetic ions such as Mg, Li and Ti, thereby partially diluting the magnetic ion (Mn). The effect of oxygen partial pressure on resistivity and MR is also studied. It is interesting to note that when $LaMnO_3$ has 24% of Mn^{4+} ions, the δ value is around 0.12. When 20% of Mn is substituted with Mg ions, i.e. $LaMn_{0.8}Mg_{0.2}O_{3+\delta}$, the concentration of Mn^{4+} ions increases to 29% and the δ value is only 0.045. As δ increases, according to [5], there will be large concentrations of La and Mn vacancies in equal amounts and this is represented generally as $La_{3/3+\delta}Mn_{3/3+\delta}O_3$

0953-8984/00/357747+12$30.00 © 2000 IOP Publishing Ltd

instead of $LaMnO_{3+\delta}$. Therefore, $LaMnO_{3.12}$ consists of almost 4% of each La and Mn vacancies. $LaMn_{0.8}Mg_{0.2}O_{3+\delta}$ samples have low δ value with high concentration of Mn^{4+} ions (29%). There are only 1% of La and Mn vacancies. There is a sharp decrease (∼74%) in the concentration of vacancies in comparison to $LaMnO_{3.12}$ and this results in decreasing vacancy scattering of holes. The reduced scattering and the enhanced concentration of Mn^{4+} ions with x ($LaMn_xM_xO_{3+\delta}$) increase the electrical conductivity. It also enhances the long-range double exchange magnetic interaction in comparison to $LaMnO_{3+\delta}$ samples. The resistivity, thermopower and magnetoresistance studies of the diamagnetic ion substituted $LaMnO_3$ are presented. Substitution of these ions in $Pr_{1-x}(Ca/Sr)_xMnO_3$ in the Mn site decreases the magnetic transition temperature, T_c and increases the magnitude of resistivity [6, 7].

2. Experiment

$LaMn_{1-x}M_xO_{3+\delta}$ (M = Li, Mg and Ti) compounds were prepared through a wet-chemical method involving a redox reaction. MnO_2 was precipitated from the reaction of $KMnO_4$ with $MnSO_4.H_2O$ salts in acidic medium in the presence of La metal ions, which were then precipitated completely by raising the pH to 7. The precipitate was filtered and washed with deionized water and decomposed at 1123 K obtaining phase-pure specimens. The details of the method were given in [8–10]. These compounds were pressed into discs and sintered in air for 5 h at 1550 K and used for electrical and magnetic measurements. X-ray diffraction (XRD) patterns were obtained using a Scintag (USA) diffractometer. The ferromagnetic transition temperatures were obtained from the dc susceptibility measurements using the Gouy method [11]. Electrical resistivity, $\rho(T)$, was measured using the two- or four-probe dc technique. The concentration of Mn^{4+} was determined by iodometric titrations using sodium thiosulphate [12]. The thermopower measurements were carried out using a dc technique by supplying heat at one side of a sintered bar and measuring the resulting thermo-emf and the differential temperature. The sintered bar is kept in between two copper electrodes and the thermopower of the sample was measured relative to copper electrodes and the absolute value is obtained by correcting for the thermopower of copper. The temperature difference (ΔT) between two ends of the sample was maintained around 2–3 K throughout the measuring procedure and measured using two copper–constantan thermocouples mounted inside copper electrodes.

3. Results

3.1. XRD studies

Aliovalent diamagnetic ions (Li, Mg and Ti) were substituted for Mn in $LaMnO_3$. The various compositions studied are $LaMn_{1-x}Mg_xO_{3+\delta}$ ($x = 0$, 0.05, 0.1, 0.2 and 0.4), $LaMn_{1-x}Li_xO_{3+\delta}$ ($x = 0.05$ and 0.1) and $LaMn_{0.95}Ti_{0.05}O_{3+\delta}$. All the prepared compositions are of single phasic nature. $LaMnO_{3+\delta}$ samples exhibit rhombohedral symmetry. Figure 1 shows the XRD pattern of $LaMnO_{3+\delta}$, $LaMn_{0.8}Mg_{0.2}O_{3+\delta}$ and $LaMn_{0.9}Li_{0.1}O_{3+\delta}$. The crystalline symmetry and the lattice parameters are given for different compositions in table 1. The iodometric titrations were carried out for the as-sintered samples. $LaMnO_{3+\delta}$ shows a large concentration of holes (24%). The concentration of Mn^{4+} ions, δ and the La, Mn vacancies for different compositions are given in table 1. The as-sintered $LaMnO_3$ samples exhibit a δ value of 0.12 and 3.85% each of La and Mn vacancies. All the other compositions show low δ and vacancy concentrations. The $LaMn_{1-x}M_xO_{3+\delta}$ (M = Li, Mg and Ti) samples also have high concentration of Mn^{4+} ions in the Mn sublattice, thus increasing the oxygen content.

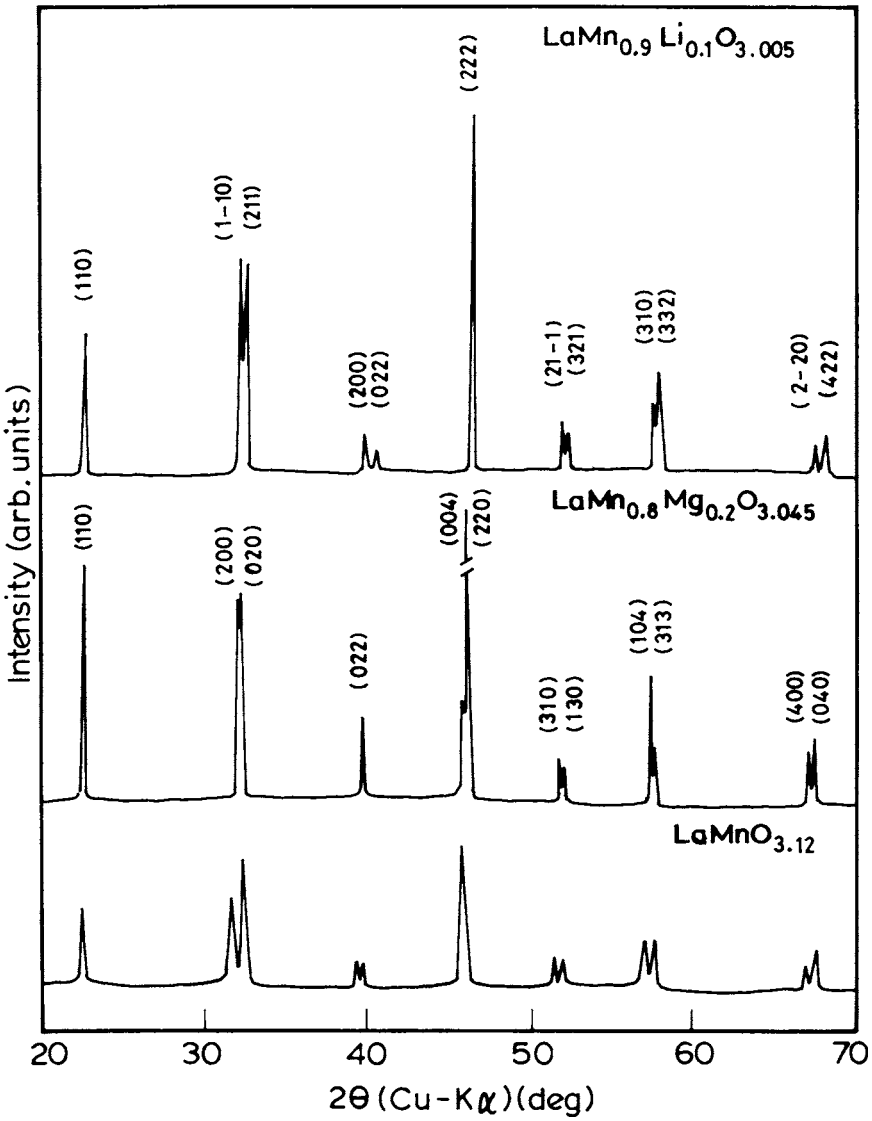

Figure 1. XRD traces of $LaMnO_{3.12}$, $LaMn_{0.8}Mg_{0.2}O_{3.045}$ and $LaMn_{0.9}Li_{0.1}O_{3.005}$.

3.2. Magnetic susceptibility

The reciprocal mass susceptibility is plotted against temperature in figure 2. All curves satisfy the Curie–Weiss relation, $\chi = C/(T - T_c)$, where C is the Curie constant. The T_c values are obtained from the fit and show an increase with diamagnetic addition. The T_c values are presented in table 1. It indicates that the smaller amount of cation vacancies and the increasing hole concentration enhance the magnetic exchange interaction.

Table 1. Crystal symmetry, lattice parameters, concentration of Mn^{4+} ions, δ, concentration of La, Mn vacancies and magnetic transition temperatures are tabulated for different $LaMn_{1-x}M_xO_{3+\delta}$ (M = Mg, Li, Ti) compositions.

Compositions	Crystal symmetry	Lattice parameters	Conc. of Mn^{4+} ions (1150 K) (%)	δ	La, Mn vacancies (%)	T_c (K)
$LaMnO_{3+\delta}$	Rhombohedral	$a = 5.560$ Å $\alpha = 60.5^\circ$	24	0.12	3.85	150
$LaMn_{0.95}Mg_{0.05}O_{3+\delta}$	Orthorhombic	$a = 5.515$ Å $b = 5.502$ Å $c = 7.880$ Å	9	0.02	<1	155
$LaMn_{0.9}Mg_{0.1}O_{3+\delta}$	Orthorhombic	$a = 5.515$ Å $b = 5.530$ Å $c = 7.899$ Å	19	0.045	1.5	170
$LaMn_{0.8}Mg_{0.2}O_{3+\delta}$	Orthorhombic	$a = 5.515$ Å $b = 5.544$ Å $c = 7.901$ Å	29	0.045	1.5	210
$LaMn_{0.9}Li_{0.1}O_{3+\delta}$	Rhombohedral	$a = 5.480$ Å $\alpha = 60.6^\circ$	20	0.005	1	185
$LaMn_{0.95}Ti_{0.05}O_{3+\delta}$	Orthorhombic	$a = 5.514$ Å $b = 5.502$ Å $c = 7.879$ Å	7	0.06	2	152

Table 2. Activation energy and room temperature resistivity for $LaMn_{1-x}M_xO_{3+\delta}$ (M = Mg, Li) compositions.

Compositions	E_a (meV) from $\log(\rho/T)$ versus $1/T$	Resistivity coefficient B (10^{-6} Ω cm K^{-1})	Room temperature resistivity (Ω cm)
$LaMnO_{3+\delta}$	231	153	368
$LaMn_{0.95}Mg_{0.05}O_{3+\delta}$	172	80	19
$LaMn_{0.9}Mg_{0.1}O_{3+\delta}$	178	20	8
$LaMn_{0.8}Mg_{0.2}O_{3+\delta}$	184	13	6
$LaMn_{0.95}Li_{0.05}O_{3+\delta}$	127	67	2.4

3.3. Resistivity

Figure 3 presents the $\rho(T)$ characteristics of Mg, Li and Ti substituted $LaMnO_3$ samples. The inset shows the $\rho(T)$ relation of $LaMnO_{3.12}$. All compositions exhibit an insulating behaviour throughout the range of temperature measurements. The diamagnetic ion addition in $LaMnO_3$ (low δ values in $LaMn_{1-x}M_xO_{3+\delta}$) does not alter the semiconducting electrical behaviour observed in $LaMnO_{3.12}$; only the magnitude of $\rho(T)$ decreases, which is ∼100–800 Ω cm up to 150 K and starts increasing to very high values at lower temperatures. Li substituted samples show lower resistivity in comparison to Mg and Ti addition. All the $\rho(T)$ curves of $LaMn_{1-x}Mg_xO_{3+\delta}$ ($x = 0.05$–0.4) show similar behaviour but they show difference in the room temperature (RT) resistivity values. For low concentrations ($x \leqslant 0.2$) of Mg, ρ(RT), decreases and these values are given in table 2. However, as x further increases, the magnitude of resistivity increases as in the case of $LaMn_{0.6}Mg_{0.4}O_3$. This may be due to the reduction in nearest neighbour interaction between Mn ions and the large decrease in the effective magnetic moment. The sintered disc of $LaMn_{0.8}Mg_{0.2}O_{3+\delta}$ shows 29% of hole concentration; however, it does not exhibit a metallic transition at lower temperatures. In

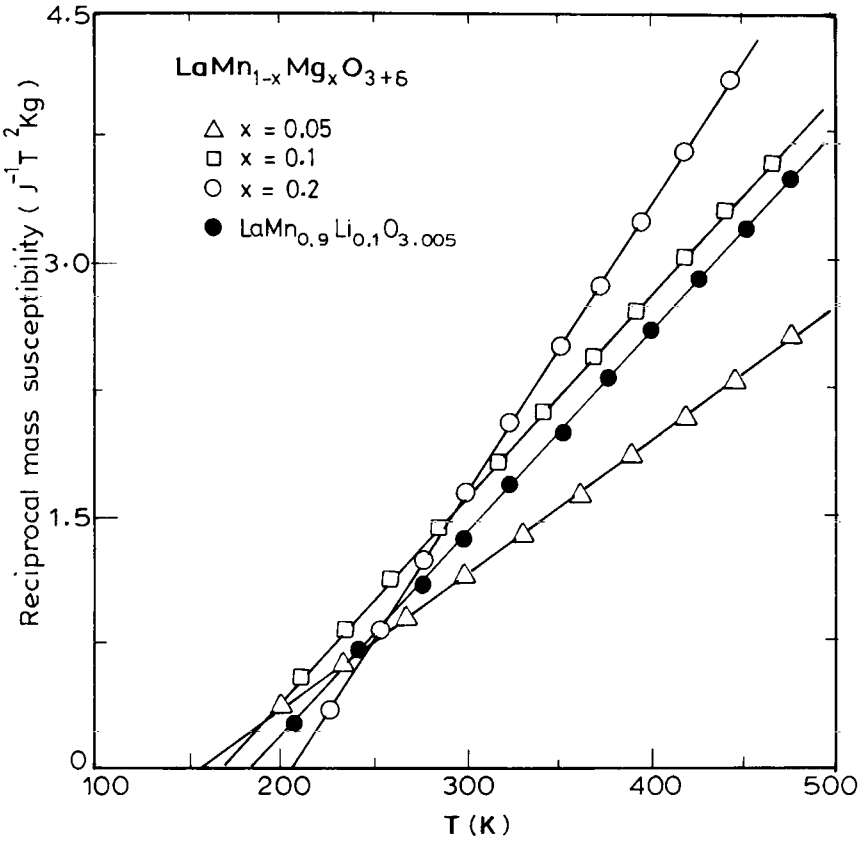

Figure 2. Reciprocal mass susceptibility is plotted against temperature for different $LaMn_{1-x}M_xO_{3+\delta}$ (M = Mg, Li) samples.

comparison, $LaMnO_3$ substituted with divalent ions (Ca, Sr and Ba) in the La site displays a ferromagnetic metallic ground state [13]. $La_{0.75}Ca_{0.25}MnO_3$ also has almost the same hole concentration as $LaMn_{0.8}Mg_{0.2}O_{3+\delta}$. However, the former is highly conductive and transforms to a metallic state below 240 K. This indicates that there exists a considerable difference between the effect of substitution in A or B sites in $LaMnO_3$ perovskite structure with ions having fixed oxidation states. The Mn ions are responsible for the electrical and magnetic properties of substituted lanthanum manganites. In the case of diamagnetic addition in the Mn sites, we are dispersing the Mn ions and thereby reducing the effective nearest neighbour interaction between Mn ions. Much of the study is on Mg or Li added specimens, because these compositions have shown larger hole concentrations in comparison to the samples with Ti addition.

Figure 4 displays the $\log(\rho/T)$ versus $(1/T)$ plots for different compositions. These curves exhibit two segments with different slopes indicating a phase transformation. There is a change-over from the paramagnetic insulating to ferromagnetic insulating state. In the high temperature segment, the curves are fitted with the small polaron resistivity expression and the activation energies are given in table 2. The small polaron resistivity expression is given

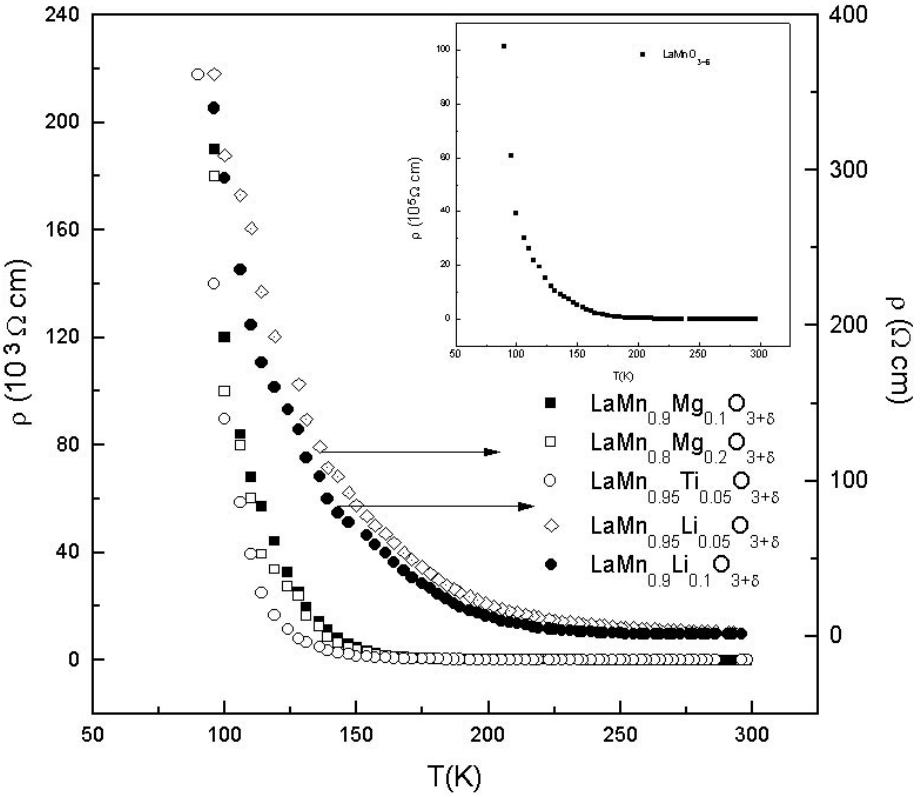

Figure 3. The resistivity, $\rho(T)$ is plotted against T for various $LaMn_{1-x}M_xO_{3+\delta}$ (M = Mg, Li, Ti) compositions. The inset shows the resistivity behaviour of $LaMnO_{3+\delta}$.

below:

$$\rho(T) = BT \exp\left(\frac{E_a}{k_B T}\right) \tag{1}$$

where E_a is the activation energy, k_B is the Boltzmann constant and B is the resistivity coefficient. The small polaron activation energy obtained experimentally for lanthanum calcium manganites is less than 0.3 eV [14]. We calculate the resistivity coefficient B from the small polaron model for $LaMn_{1-x}Mg_xO_{3+\delta}$ ($x = 0, 0.05, 0.1$ and 0.2) and $LaMn_{0.95}Li_{0.05}O_{3+\delta}$ and it is presented in table 2. The value of B decreases with increase in x. According to the Emin–Holstein [15] small polaron hopping model,

$$B = g_d k_B / n e^2 \alpha^2 \nu_0 \tag{2}$$

where e is the electronic charge, α is the hopping distance, n is the polaron concentration and ν_0 is a characteristic frequency of the longitudinal optical phonon that carries the polaron through the lattice. The factor g_d depends on lattice geometry and has the value 3/2 for triangular lattice and 1 for nearest neighbour hopping on a square planar lattice. Mg^{2+}, Li^+ and Ti^{4+} substituted in the Mn site are not Jahn–Teller ions; they have a filled outer orbital and are diamagnetic ions. Substitution of these ions replaces Mn^{3+} in $LaMnO_3$ thus reducing the lattice distortion. The two factors which alter B significantly are n and α. As presented in table 2, the value of B decreases from $x = 0$ to 0.2 unlike what is observed in Ga and Al doped

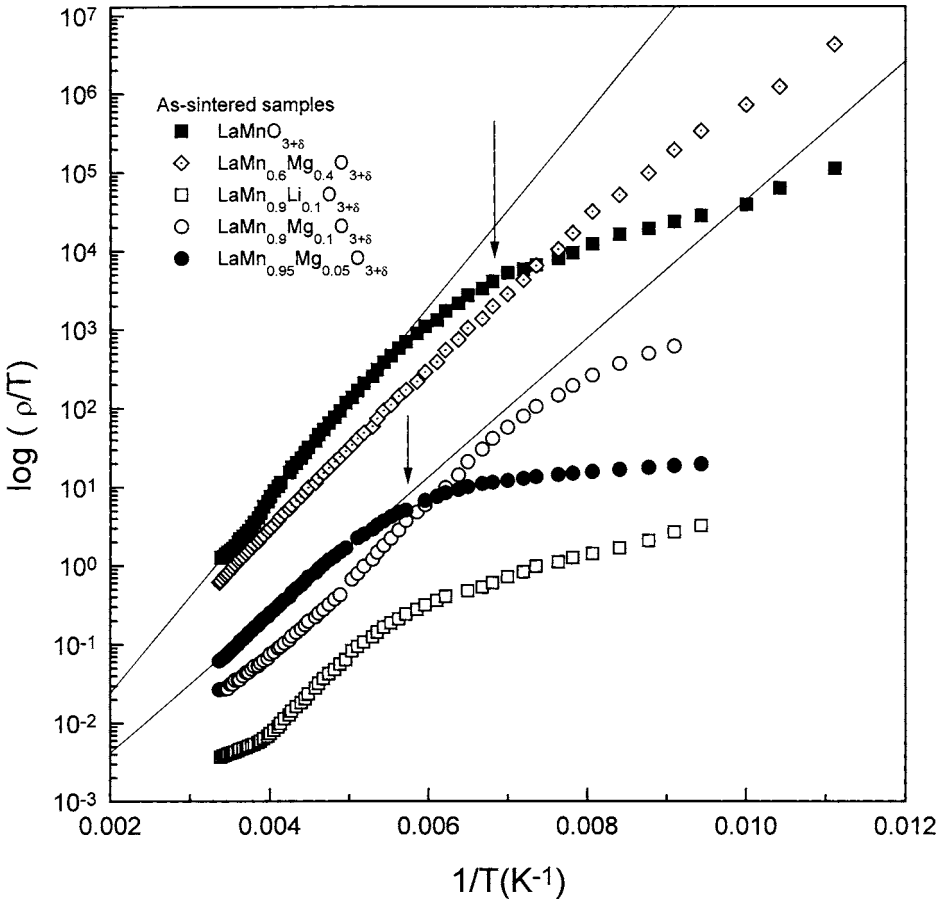

Figure 4. The $\log(\rho/T)$ versus $1/T$ plots for different $LaMn_{1-x}M_xO_{3+\delta}$ (M = Mg, Li) compositions (arrows indicate the temperatures corresponding to the change in slope, two curves are fitted with small polaron resistivity relation at high temperatures).

$La_{0.67}Ca_{0.33}Mn_{1-x}(Ga/Al)_xO_3$. From the calculated B values, it is evident that even at higher diamagnetic concentrations the hopping distance is the dominant factor. When x is raised, the concentration of holes increases, as in the case of $LaMn_{0.8}Mg_{0.2}O_{3+\delta}$ (Mn^{4+} = 29%); however, the lattice distortion is greatly reduced, consequently decreasing the polaron number n. The drop in n may not be sufficient to lower the product $n\alpha^2$ to enhance the value of B. In $La_{0.67}Ca_{0.3}Mn_{1-x}Ga_xO_3$, the resistivity coefficient decreases for low levels of Ga ($x = 0.02, 0.05$) doping; however, when x is raised, there is a significant increase in B. Young Sun *et al* [16] attributed it to the significant reduction in polaron concentration, n, at high x values leading to small magnitude for the product $n\alpha^2$ in equation (2).

The ρ–T characteristics of $LaMnO_{3+\delta}$ and $LaMn_{0.8}Mg_{0.2}O_{3+\delta}$ samples after treating in low partial pressures of O_2 ($p_{O_2} \sim 10^{-8}$ to 10^{-10} atm) at 1373 K are shown in figure 5. The as-sintered samples ($\delta = 0.07$ to 0.15) show a large decrease in oxygen content, thereby increasing the resistivity. There is almost one order increase in $\rho(T)$, indicating reduction in holes and effective magnetization. These two changes drastically affect the resistivity characteristics. The change in slope observed in the as-sintered $LaMnO_{3+\delta}$ is not observed in samples annealed in lower p_{O_2} atmospheres. Annealing modifies the ferromagnetic behaviour and transforms

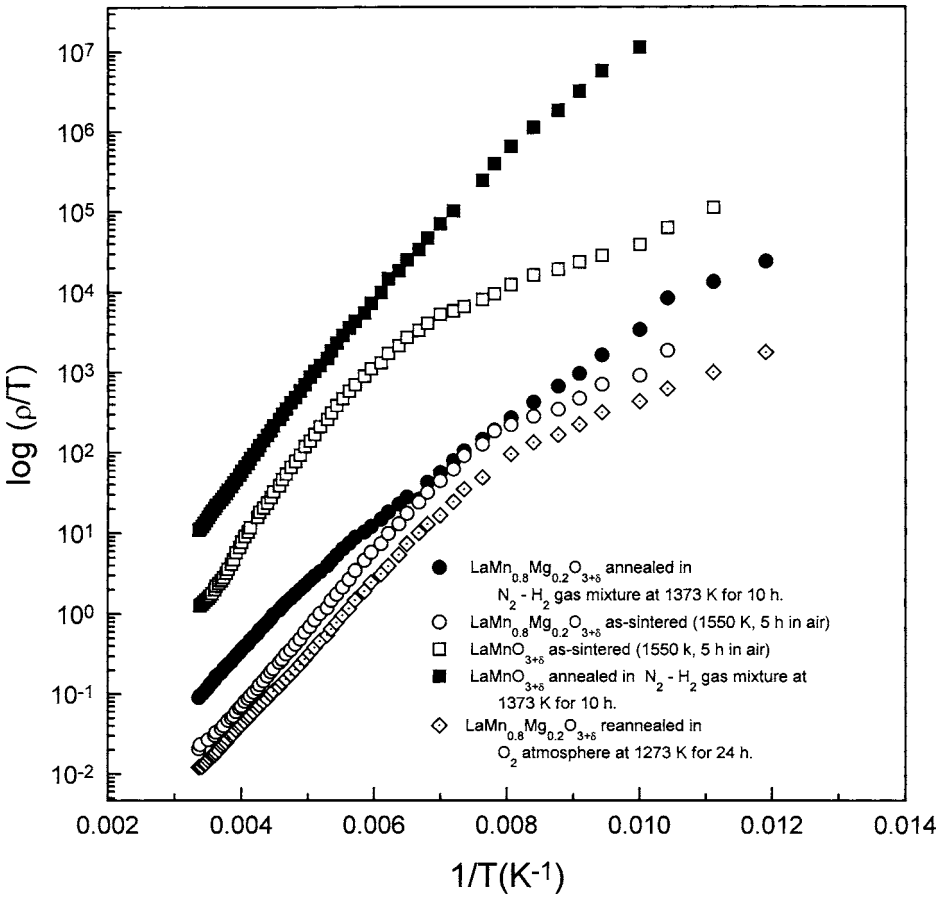

Figure 5. The $\log(\rho/T)$ versus $1/T$ plots for $LaMnO_{3+\delta}$ and $LaMn_{0.8}Mg_{0.2}O_{3+\delta}$ compositions treated in N_2–H_2 and O_2 atmosphere.

to antiferromagnetic phase. The concentration of holes in $LaMn_{0.8}Mg_{0.2}O_{3+\delta}$ has reduced to 21% after annealing in lower p_{O_2}. Reannealing of the $LaMn_{0.8}Mg_{0.2}O_3$ sample treated in low p_{O_2} in oxygen increases the hole concentration to 29% and thereby reducing the resistivity.

3.4. Thermopower

Thermopower, $S(T)$, against T is plotted in figure 6 for Mg added $LaMnO_3$ samples ($x = 0.05, 0.2$). The curves show increased S when the temperature is lowered below 298 K indicating an insulating state. However, at some critical temperature, they exhibit a peak in S and with further decrease in temperature, S starts decreasing, which is characteristic of metallic samples. However, this is contrary to what is observed in the resistivity behaviour according to which there is no transition to a metallic state at low temperature. Similar behaviour is observed in ferromagnetic insulating $La_{0.82}Ca_{0.18}MnO_3$ samples, which show a decreasing trend in S below T_c [14]. The peak in S observed in $LaMn_{1-x}Mg_xO_{3+\delta}$ is around the magnetic transition temperature obtained from the dc susceptibility data shown in table 1. One feature that requires special attention is the peak exhibited by S near T_c. This may arise from the magnetic specific heat (ΔC_m) anomaly near the magnetic transition. If the holes have strong

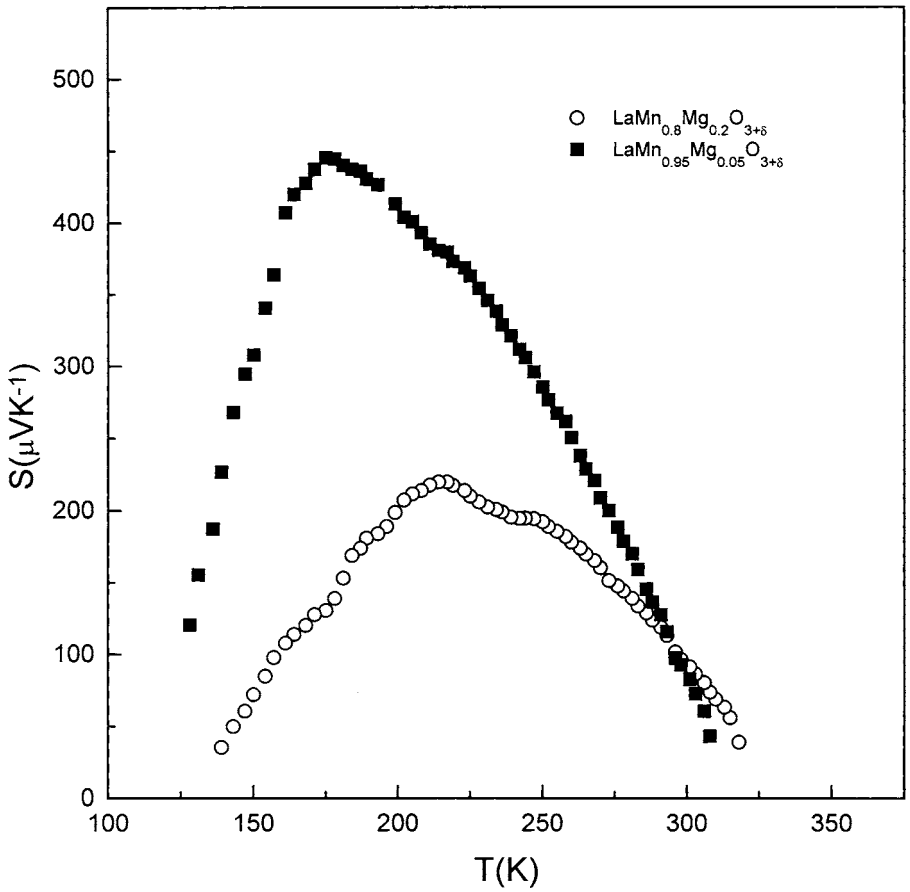

Figure 6. Thermopower, $S(T)$, versus temperature for $LaMn_{1-x}Mg_xO_{3+\delta}$ ($x = 0.05, 0.2$).

coupling to the magnetic spins, a part of the entropy can be transferred to the entropy of the holes, much like the phonon drag effect. The relation between S and the magnetic specific heat is $S = \frac{1}{3}(\eta \Delta C_m/|e|N)$ [17, 18] where N is the hole concentration and η is a measure of the coupling of the spin entropy to the entropy of carriers. Thus S decreases with decrease in ΔC_m and increase in N.

3.5. Magnetoresistance

Magnetoresistance (MR) is defined as $MR_H = (\rho(0) - \rho(H))/\rho(0)$, where $\rho(0)$ is the resistivity at zero field and $\rho(H)$ is the resistivity at the field H. MR_H versus T is plotted in figure 7. MR curves of $LaMn_{1-x}Mg_xO_3$ ($x = 0.05$–0.2) are only shown in detail because these compositions exhibited large negative MR at low magnetic fields ($H = 1$ T). As the Mg concentration increases, the MR coefficient increases and becomes sharper. $LaMn_{0.95}Mg_{0.05}O_{3+\delta}$ exhibits the MR peak around 125 K; however, the other two samples ($x = 0.1$ and 0.2) display peaks around 150 K. The difference in T_c and the temperature corresponding to the maximum of MR may be due to the canted nature of the spins. The large negative MR may arise as a result of the reduction in vacancies and the enhanced hole concentration. The reduced vacancies enhance the long-range double-exchange magnetic

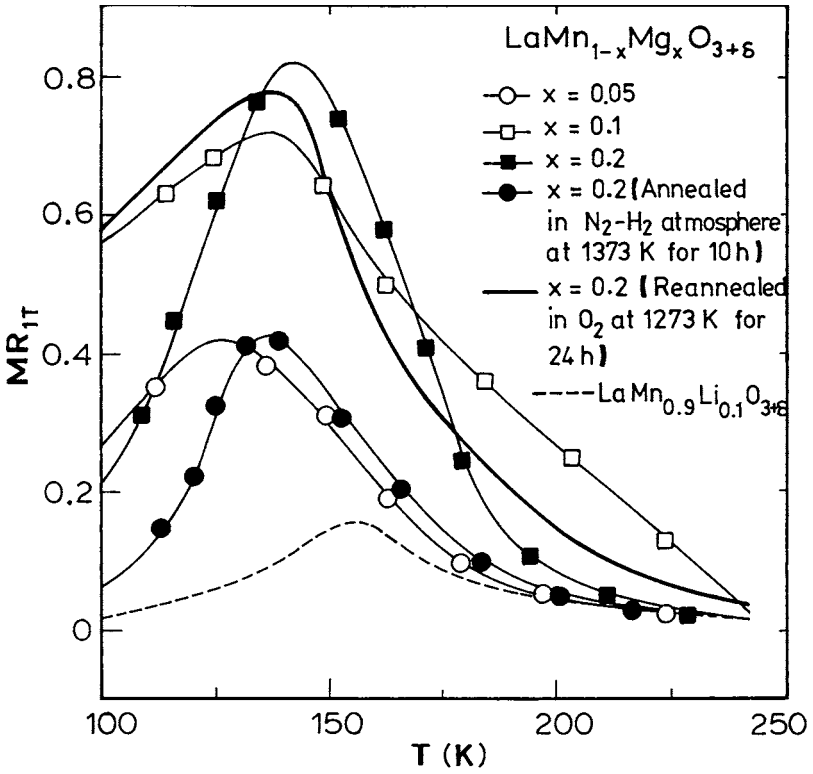

Figure 7. Magnetoresistance (MR) versus temperature plots for $LaMn_{1-x}M_xO_{3+\delta}$ (M = Li, Mg).

interaction. In [13] it is reported that $La_{0.75}Ca_{0.25}MnO_3$ exhibits an MR of 0.8 at a magnetic field of 4 T. The $LaMn_{0.8}Mg_{0.2}O_3$ sample treated at low p_{O_2} shows low MR due to reduction in Mn^{4+} ions in the system. Reannealing of $LaMn_{0.8}Mg_{0.2}O_3$ samples treated in lower p_{O_2} atmosphere increases the hole concentration and thus exhibits larger MR. $LaMn_{0.9}Li_{0.1}O_{3+\delta}$ shows low MR coefficient in comparison to Mg added samples.

4. Discussion

The aliovalent diamagnetic ion substitutions in the Mn sublattice in $LaMnO_3$ decrease the resistivity and exhibit large negative MR at low temperatures. The MR increases with x ($x = 0.05$–0.2). Thermopower measurements display a change in behaviour indicating a modified magnetic state at low temperature. The iodometric titration results indicate the presence of Mn^{4+} ions in the Mn sublattice. Thus the addition of Mg and Li ions increases Mn^{4+} concentration and decreases the $\rho(RT)$ values. However, samples with larger Mg or Li concentration (large concentration of Mn^{4+} ions) do not exhibit a metallic state at low temperature; instead, they display the resistivity behaviour of localized charge carriers. One factor which may influence the resistivity is the occupation of the Mn site by diamagnetic ions. As a result of the formation of Mn^{3+}–O–M–O–Mn^{4+} (M = Li^+, Mg^{2+}, Ti^{4+}), the hopping distance of the hole from the Mn^{4+} to Mn^{3+} ion increases and thereby reduces the hopping probability as well as the mobility of the charge carriers. Jaime *et al* [19] suggested that the small polarons not only hop among nearest neighbour sites, but also across the face diagonals.

In such next nearest neighbour interactions there will be deviations of the Mn–O–Mn bond angle from 180°. Worledge *et al* [20] argued that polarons could hop more than nearest neighbour sites considering the on-site Coulomb repulsion and the effects of polaron–polaron interactions. The magneto-electrical properties of manganites have traditionally been examined within the framework of double exchange (DE), which considers the magnetic coupling between the two partially filled d shells with strong on-site Hund coupling. In the DE mechanism, the Mn–O–Mn bond angle is assumed to be 180° in a typical cubic crystal system. The decrease in Mn–O–Mn angle reduces the matrix element b, which describes the hole hopping between Mn sites. Considering the case of $LaMn_{1-x}M_xO_{3+\delta}$, if we consider the next nearest neighbour interaction then the hopping distance increases and the Mn–O–Mn bond angle decreases, resulting in reduced hopping between Mn^{4+} and Mn^{3+}. The diamagnetic ions Li^+, Mg^{2+} have filled shells and act as barriers due to strong on-site Coulomb repulsion to the charge carriers that try to occupy these sites. Only charge carriers with sufficient energy can hop over the diamagnetic ions in the Mn^{4+}–O–M–O–Mn^{3+} configuration, whereas the carriers with lower energy try to localize around the Mn sites. This effect may enhance the resistance at lower temperature and the transition to a metallic state can be suppressed. The calculated resistivity coefficient B confirms that the hopping distance is the prominent factor that influences the resistivity characteristics. The ferromagnetic state observed at low temperature does not greatly affect the electrical transport properties. We observe only slight changes in slope in the resistivity curves below T_c.

5. Conclusions

Addition of diamagnetic ions in the Mn sublattice in $LaMnO_3$ enhances the Mn^{4+} concentration. The presence of diamagnetic ions between Mn^{3+} and Mn^{4+} increases the hole hopping distance. The large MR is observed only for Mg substituted samples. Mg differs from the other diamagnetic ions in the oxidation state and the ionic size. Low δ values observed in $LaMn_{1-x}M_xO_{3+\delta}$ do not modify the electrical properties, thus the insulating state is observed for all the compositions. The high temperature resistivity behaviour can be fitted with the small polaron model. The activation energy calculated from the fitted curves has a magnitude less than 0.3 eV. Samples treated at low partial pressures of oxygen show increases in resistivity and the MR coefficient also reduces. Reannealing of the same samples in oxygen regains the Mn^{4+} ions and they exhibit the resistivity and MR behaviour as the original sample.

Acknowledgment

One of the authors (JP) is grateful to the Council of Scientific and Industrial Research, New Delhi for providing financial support through a research fellowship.

References

[1] Wollan E O and Kochler K C 1955 *Phys. Rev.* **100** 545
[2] Ritter C, Ibarra M R, De Teresa J M, Algarabel P A, Marquina C, Blasco J, Garcia J, Oseroff S and Cheon S W 1997 *Phys. Rev.* B **56** 8902
[3] Ghivelder L, Abrego Castillo I, Gusmao M A, Alonso J A and Cohen L F 1999 *Phys. Rev.* B **60** 12 184
[4] Skumryev V, Ott F, Coey J M D, Anane A, Renard J P, Pinsard-Guaudart L and Revcolevschi A 1999 *Eur. Phys. J.* B **11** 401
[5] Van Roosmalen J A M, Cordfunke E H P, Helmholdt R B and Zandbergen H W 1994 *J. Solid State Chem.* **110** 100
[6] Maignan A and Raveau B 1997 *Z. Phys.* B **102** 299

[7] Maignan A, Martin C and Raveau B 1997 *Z. Phys.* B **102** 19
[8] Philip J and Kutty T R N 1999 *Mater. Lett.* **39** 311
[9] Philip J and Kutty T R N 2000 *Mater. Phys. Chem.* **63** 218
[10] Philip J and Kutty T R N 1999 *J. Phys.: Condens. Matter* **11** 8537
[11] Crangle J 1977 *The Magnetic Properties of Solids* (London: Arnold) p 161
[12] Vogel I 1989 *Textbook of Quantitative Chemical Analysis* (Essex: Addison Wesley Longman) p 384
[13] Schiffer P, Ramirez A P, Bao W and Cheong S W 1995 *Phys. Rev. Lett.* **75** 3336
[14] Hundley M F and Neumeier J J 1997 *Phys. Rev.* B **55** 11 511
[15] Emin D and Holstein T 1969 *Ann. Phys., NY* **53** 439
[16] Sun Young, Xu Xiaojun, Zheng Lei and Zhang Yuheng 1999 *Phys. Rev.* B **60** 12 317
[17] Mahendiran R, Tiwary S K, Raychaudhari A K, Ramakrishnan T V, Mahesh R, Rangavittal N and Rao C N R 1996 *Phys. Rev.* B **53** 3348
[18] Jan J P 1957 *Solid State Phys.* **5** 1
[19] Jaime M, Hardner H T, Salamon M B, Rubinstein M, Dorsey P and Emin D 1997 *Phys. Rev. Lett.* **78** 951
[20] Worledge D C, Mieville L and Geballe T H 1998 *Phys. Rev.* B **57** 15 267